

# Observability of dynamical networks from graphic and symbolic approaches

Irene Sendiña-Nadal<sup>1,2</sup>[0000-0003-0432-235X],  
and Christophe Letellier<sup>3</sup>[0000-0003-3603-394X]

- <sup>1</sup> Complex Systems Group & GISC, Universidad Rey Juan Carlos, 28933 Móstoles, Madrid, Spain [irene.sendina@urjc.es](mailto:irene.sendina@urjc.es)  
<sup>2</sup> Center for Biomedical Technology, Universidad Politécnica de Madrid, 28223 Pozuelo de Alarcón, Madrid, Spain  
<sup>3</sup> Normandie Université CORIA, Campus Universitaire du Madrillet, F-76800 Saint-Etienne du Rouvray, France [christophe.letellier@coria.fr](mailto:christophe.letellier@coria.fr)

**Abstract.** A dynamical network, a graph whose nodes are dynamical systems, is usually characterized by a large dimensional space which is not always accesible due to the impossibility of measuring all the variables spanning the state space. Therefore, it is of the utmost importance to determine a reduced set of variables providing all the required information for non-ambiguously distinguish its different states. Inherited from control theory, one possible approach is based on the use of the observability matrix defined as the Jacobian matrix of the change of coordinates between the original state space and the space reconstructed from the measured variables. The observability of a given system can be accurately assessed by symbolically computing the complexity of the determinant of the observability matrix and quantified by symbolic observability coefficients. In this work, we extend the symbolic observability, previously developed for dynamical systems, to networks made of coupled  $d$ -dimensional node dynamics ( $d > 1$ ). From the observability of the node dynamics, the coupling function between the nodes, and the adjacency matrix, it is indeed possible to construct the observability of a large network with an arbitrary topology.

**Keywords:** Dynamical network · Observability

## 1 Introduction

Consider a network composed of  $N$  nodes each one of them having a  $d$ -dimensional dynamics and whose interactions are given by an adjacency matrix  $A$ . We can thus distinguish three levels of description of this network: i) the node dynamics using the corresponding  $d \times d$  node Jacobian matrix  $\mathcal{J}_n$ , ii) the topology described by the  $N \times N$  adjacency matrix  $A$ , and iii) the whole dynamical network described by the  $d \cdot N \times d \cdot N$  network Jacobian matrix  $\mathcal{J}_N$ . There are two possible conventions for writing the adjacency matrix, one being the transposed of the other. In order to do this without unnecessary complicated notations, we will

retain the convention used by Newman [12] in which each element  $A_{ij}$  of the adjacency matrix  $A$  corresponds to an edge from node  $j$  to node  $i$ .

The node Jacobian matrix  $\mathcal{J}_n$ , computed from the set of the  $d$  differential equations governing the node dynamics, allows an easy construction of the fluence graph describing how the  $d$  variables of the node dynamics are interacting. Such fluence graphs were used by Lin for assessing the controllability of linear systems [9] and later on the theory was extended to address their observability [2]. When dealing with dynamical networks it is important to distinguish the adjacency matrix  $A$  from the network Jacobian matrix  $\mathcal{J}_N$  since, very often the observability of a network has been wrongly investigated by only taking into account the adjacency matrix [1,3,15] and disregarding the node dynamics. We show how such an approach does not always provide correct results.

Without loss of generality, we will exemplify our methodology to assess the observability of dynamical networks by considering networks of diffusively coupled Rössler systems [13] ( $d = 3$ ). The knowledge gathered from the analysis of dyads and triads of Rösslers will guide us to propose some rules to handle larger networks in a systematic way by decomposing the networks in blocks whose observability properties is known. In order to select a reduced set of variables we will use a graphical approach by introducing a pruned fluence graph of the network Jacobian matrix  $\mathcal{J}_N$  as developed in [7]. Then, the symbolic observability coefficients are computed as detailed in [8] and, when full observability is detected, the analytical determinant of the observability matrix is checked to rigorously validate the graphical and symbolic results.

## 2 Theoretical background

### 2.1 Observability matrix

Let us consider a  $d \cdot N$ -dimensional network  $\mathcal{N}$  composed of  $N$  nodes each one having an associated  $d$ -dimensional dynamics. The network state is represented by the state vector  $\mathbf{x} \in \mathbb{R}^{d \cdot N}$  whose components are given by

$$\dot{x}_i = f_i(x_1, x_2, x_3, \dots, x_{d \cdot N}), \quad (i = 1, 2, \dots, d \cdot N) \quad (1)$$

where  $f_i$  is the  $i$ th component of the vector field  $\mathbf{f}$ . The corresponding network Jacobian matrix  $J_{ij} = \frac{\partial f_i}{\partial x_j}$ , can be expressed as

$$\mathcal{J}_N = \mathbb{I}_N \otimes \mathcal{J}_n - \rho(L \otimes H) \quad (2)$$

reflecting its structure in  $N$  diagonal blocks containing the node Jacobian matrix  $\mathcal{J}_n$ . The second term corresponds to the contribution to the network dynamics from the topology encoded in the Laplacian matrix  $L = (L_{ij}) = (A_{ij} - k_i \delta_{ij})$  and the linear coupling function  $H \in \mathbb{R}^{d \times d}$ .  $\mathbb{I}_N$  is the square identity matrix of size  $N$ , the symbol  $\otimes$  stands for the Kronecker product and  $\rho$  is the coupling constant.

Let us introduce the measurement vector  $h(\mathbf{x}) \in \mathbb{R}^m$  whose  $m$  components are the measured variables. The observability cannot be stated only from these

$m$  measured variables. Indeed, to construct the observability matrix  $\mathcal{O}$  of the network dynamics from these  $m$  measured variables, it is also necessary to specify the  $d_r - m$  variables required for completing the vector  $\mathbf{X} \in \mathbb{R}^{d_r}$  spanning the reconstructed space in which the dynamics is investigated. For these reasons, and as introduced by Lin [9], we will speak about the observability of the pair  $[\mathcal{J}_N, \mathbf{X}]$  to explicit the fact that the network described by  $\mathcal{J}_N$  is observable *via* the  $m$  measured variables and  $d_r - m$  of their derivatives. Since we are interested in the smallest state space in which the dynamics can be investigated, we will limit ourselves to the case where  $d_r = d \cdot N$ .

The observability of a dynamical network can be defined as follows. Let us consider the case when  $m = 1$  (a generalization to larger  $m$  is straightforward), and let  $\mathbf{X} \in \mathbb{R}^{d \cdot N}$  be the vector spanning the reconstructed space obtained by using the  $(d \cdot N - 1)$  successive Lie derivatives of the measured variables. The dynamical system (1) is said to be *state observable* at time  $t_f$  if every initial state  $\mathbf{x}(0)$  can be uniquely determined from the knowledge of a finite time series  $\{\mathbf{X}\}_{\tau=0}^{t_f}$ . In practice, it is possible to test whether the pair  $[\mathcal{J}_N, \mathbf{X}]$  is observable by computing the rank of the observability matrix [4], that is, the Jacobian matrix of the Lie derivatives of  $h(\mathbf{x})$ .

Differentiating the measured vector  $h(\mathbf{x})$  yields  $\frac{d}{dt}h(\mathbf{x}) = \frac{\partial h}{\partial \mathbf{x}}\mathbf{f}(\mathbf{x}) = \mathcal{L}_{\mathbf{f}}h(\mathbf{x})$ , where  $\mathcal{L}_{\mathbf{f}}h(\mathbf{x})$  is the Lie derivative of  $h(\mathbf{x})$  along the vector field  $\mathbf{f}$ . The  $k$ th order Lie derivative is given by  $\mathcal{L}_{\mathbf{f}}^k h(\mathbf{x}) = \frac{\partial \mathcal{L}_{\mathbf{f}}^{k-1} h(\mathbf{x})}{\partial \mathbf{x}}\mathbf{f}(\mathbf{x})$ ,  $\mathcal{L}_{\mathbf{f}}^0 h(\mathbf{x}) = h(\mathbf{x})$  being the zeroth order Lie derivative of the measured variable itself. Therefore, the  $d \cdot N \times d \cdot N$  observability matrix  $\mathcal{O}_{\mathbf{X}}$  can be written as

$$\mathcal{O}_{\mathbf{X}}(\mathbf{x}) = \left[ dh(\mathbf{x}), d\mathcal{L}_{\mathbf{f}}h(\mathbf{x}), \dots, d\mathcal{L}_{\mathbf{f}}^{d \cdot N - 1}h(\mathbf{x}) \right]^T. \quad (3)$$

The pair  $[\mathcal{J}_N, \mathbf{X}]$  is state observable if and only if the observability matrix has full rank, that is,  $\text{rank}(\mathcal{O}_{\mathbf{X}}) = d \cdot N$ . The Jacobian matrix of the coordinate transformation  $\Phi : \mathbb{R}^{d \cdot N} \mapsto \mathbb{R}^{d \cdot N}$  between the original state space  $\mathbb{R}^{d \cdot N}(\mathbf{x})$  and the reconstructed space  $\mathbb{R}^{d \cdot N}(\mathbf{X})$  is the observability matrix  $\mathcal{O}_{\mathbf{X}}$  [6].

## 2.2 Symbolic observability coefficients

The procedure to calculate the symbolic observability coefficients is implemented in four steps as follows [8]. The first step is devoted to the construction of the symbolic Jacobian matrix  $\tilde{\mathcal{J}}_N$  by replacing each constant element  $J_{ij}$  by “1”, each non-constant polynomial element  $J_{ij}$  by “ $\bar{1}$ ”, and each rational element  $J_{ij}$  by “ $\bar{\bar{1}}$ ” when the  $j$ th variable is present in the denominator or by  $\bar{1}$  otherwise. Rational terms are distinguished from non-constant polynomial terms since they strongly reduce the observability.

The second step corresponds to the construction of the symbolic observability matrix  $\tilde{\mathcal{O}}_{\mathbf{X}}$  [8]. When  $m$  variables are measured, the construction of  $\tilde{\mathcal{O}}_{\mathbf{X}}$  is performed by blocks of size  $(\kappa_i + 1) \times d$ , being  $\kappa_i$  the number of derivatives of

the  $i$ th measured variable and  $m + \sum_{i=1}^m \kappa_i = d \cdot N$ : the construction of each block follows the same rules as introduced in [8] for univariate measures.

The third step consists in computing the symbolic observability coefficients. The determinant of  $\tilde{\mathcal{O}}_{\mathbf{X}}$  is computed according to the symbolic algebra defined in [8] and expressed as products and addends of the symbolic terms 1,  $\bar{1}$  and  $\bar{\bar{1}}$ , whose number of occurrences are stored in variables  $N_1$ ,  $N_{\bar{1}}$  and  $N_{\bar{\bar{1}}}$ , respectively. A special condition is required for rational systems such that, if  $N_{\bar{1}} = 0$  and  $N_{\bar{\bar{1}}} \neq 0$  then  $N_{\bar{1}} = N_{\bar{\bar{1}}}$ . The symbolic observability coefficient for the reconstructed vector  $\mathbf{X}$  is then equal to  $\eta_{\mathbf{X}} = \frac{1}{D}N_1 + \frac{1}{D^2}N_{\bar{1}} + \frac{1}{D^3}N_{\bar{\bar{1}}}$  with  $D = \max(1, N_1) + N_{\bar{1}} + N_{\bar{\bar{1}}}$  and  $0 \leq \eta_{\mathbf{X}} \leq 1$ , being  $\eta_{\mathbf{X}} = 1$  for a reconstructed vector  $\mathbf{X}$  providing a full observability. It was shown that the observability can be considered as being good when  $\eta_{\mathbf{X}} \geq 0.75$  [11].

### 2.3 Selecting the variables to measure

A systematic check of all the possible combinations of  $m$  measured variables and their  $d \cdot N - m$  derivatives turns out to be a daunting task for large  $N$  and large  $d$ . Therefore, it becomes crucial to furnish methods to unveil a tractable set of variables providing full observability of a system. This may be achieved by using a graphical approach [7] which is an improved version of the procedure introduced by Liu *et al.* [10]. A pruned fluence graph with  $d \cdot N$  vertices (one per variable) and a directed edge  $x_j \rightarrow x_i$  is drawn between variables  $x_j$  and  $x_i$  when the element  $J_{ij}$  of  $\mathcal{J}_N$  is constant. At least one variable from each root Strongly Connected Component (rSCC) of the pruned fluence graph has to be measured [7]. A rSCC is a subgraph in which there is a directed path from each node to every other node in the subgraph and with no *outgoing* edges. As we will see, a pruned fluence graph provides a necessary but not a sufficient reduced set of variables to measure for getting an observable pair  $[\mathcal{J}_N, \mathbf{X}]$ .

## 3 Observability of the node dynamics

The node dynamics corresponds to the Rössler system [13]  $(x_1, x_2, x_3) = (x, y, z)$  whose evolution is governed by the vector field  $(f_1, f_2, f_3) = [-y - z, x + ay, b + z(x - c)]$ , whose Jacobian matrix is

$$\mathcal{J}_n = \begin{bmatrix} 0 & -1 & -1 \\ 1 & a & 0 \\ z & 0 & x - c \end{bmatrix}. \quad (4)$$

Its nonzero constant elements  $J_{ij}$  lead to the pruned fluence graph shown in Fig. 1 which has a single rSCC (dashed oval) containing variables  $x$  and  $y$ .

Variable  $z$  can thus be discarded from measurements but, at least, variable  $x$  or  $y$  must be measured. The symbolic observability coefficients for the pair  $[\mathcal{J}_n, (x, \dot{x}, \ddot{x})]$ ,  $[\mathcal{J}_n, (y, \dot{y}, \ddot{y})]$ , and  $[\mathcal{J}_n, (z, \dot{z}, \ddot{z})]$  are  $\eta_{x\dot{x}\ddot{x}} = 0.86$ ,  $\eta_{y\dot{y}\ddot{y}} = 1.00$ , and

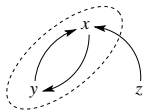


**Fig. 1.** Pruned fluence graph of the Rössler system where an edge is drawn between variables  $x_i$  and  $x_j$  whenever  $J_{ij}$  is a nonzero constant. A dashed oval surrounds the root strongly connected component (rSCC). Edges  $x_i \rightarrow x_i$  are omitted since they do not contribute to the determination of the rSCC.

$\eta_{z\dot{z}\ddot{z}} = 0.44$ , respectively. This means that the pair  $[\mathcal{J}_n, (y, \dot{y}, \ddot{y})]$  is fully observable, the observability of the pair  $[\mathcal{J}_n, (x, \dot{x}, \ddot{x})]$  is good and the pair  $[\mathcal{J}_n, (z, \dot{z}, \ddot{z})]$  is poorly observable. The pruned fluence graph returns the two variables providing the largest observability coefficients when each one of them is measured alone. This can be analytically confirmed by computing the determinants of the corresponding observability matrices which are  $\text{Det } \mathcal{O}_{x\dot{x}\ddot{x}} = x - (a + c)$ ,  $\text{Det } \mathcal{O}_{y\dot{y}\ddot{y}} = 1$ , and  $\text{Det } \mathcal{O}_{z\dot{z}\ddot{z}} = z^2$ , respectively. If  $\text{Det } \mathcal{O}_{\mathbf{X}} = 0$  for a subset  $\mathcal{M}^{\text{obs}} \subset \mathbb{R}^d$  of the state space associated with the node dynamics, then  $\mathcal{M}^{\text{obs}}$  is non observable through the measurements and it is called the singular observability manifold. Since  $\text{Det } \mathcal{O}_{y\dot{y}\ddot{y}} = 1$ ,  $\mathcal{M}^{\text{obs}}$  is an empty set, the pair  $[\mathcal{J}_n, (y, \dot{y}, \ddot{y})]$  is actually fully observable. When the reconstructed space is spanned by  $\mathbf{X} = (x, \dot{x}, \ddot{x})$ , the plane defined by  $x = a + c$  is non observable. The plane  $z = 0$  is nonobservable when  $z$  is measured. It was shown that the complexity of the determinant, assessed for instance by the order of its expression (1 for  $\text{Det } \mathcal{O}_{x\dot{x}\ddot{x}}$ , 0 for  $\text{Det } \mathcal{O}_{y\dot{y}\ddot{y}}$ , and 2 for  $\text{Det } \mathcal{O}_{z\dot{z}\ddot{z}}$ ), is related to the observability: the larger the order, the less observable the pair  $[\mathcal{J}_n, \mathbf{X}]$  [5].

## 4 Observability of small network motifs

### 4.1 Dyads ( $N = 2$ )

Let us start with a small network motif of two Rösslers bidirectionally coupled by either  $x$ ,  $y$ , or  $z$ . From the analysis of this basic motif we will derive general rules for assessing the observability of larger networks. The corresponding  $\mathcal{J}_N$  for the case the two nodes are coupled through the  $x$  variable is given by

$$\mathcal{J}_N = \left[ \begin{array}{ccc|ccc} -\rho_x & -1 & -1 & \rho_x & 0 & 0 \\ 1 & a & 0 & 0 & 0 & 0 \\ z & 0 & x - c & 0 & 0 & 0 \\ \hline \rho_x & 0 & 0 & -\rho_x & -1 & -1 \\ 0 & 0 & 0 & 1 & a & 0 \\ 0 & 0 & 0 & z & 0 & x - c \end{array} \right]$$

where  $H = H_x = [1, 0, 0; 0, 0, 0; 0, 0, 0]$  has been used in Eq. (2).

Figure 2 shows the pruned fluence graphs obtained from  $\mathcal{J}_N$  for the three coupling configurations. Below each graph, a compact representation at the level of the adjacency matrix is also provided, indicating as well the coupling nature of

the bidirectional links. There is only one rSCC when the two nodes are coupled either *via* variable  $x$  or  $y$  whereas there are two rSCCs when coupled *via* variable  $z$ . This suggests that at least one variable has to be measured among  $\{x_1, y_1, x_2, y_2\}$  in the first two cases (Figs. 2a and 2b) and one ( $x_i$  or  $y_i$ ) in each rSCC in the latter case. In the following, we will analyze in detail the cases where  $m = 1, 2$ , that is, 1 or 2 measured variables, which can be acquired in  $N_m = 1$  or 2 nodes. We computed the symbolic observability coefficients  $\eta_{\mathbf{X}}$  for all possible reconstructed vectors  $\mathbf{X}$ . A summary of these analysis is reported in Table 1.

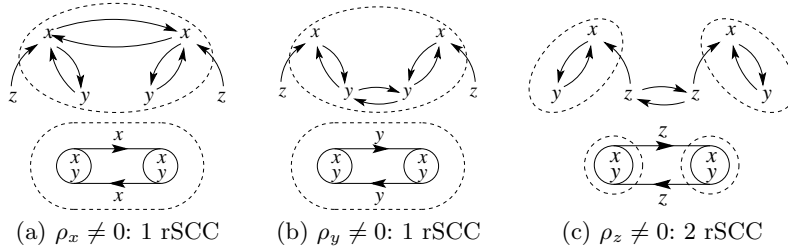


**Fig. 2.** Pruned fluence graphs (top) and network connection motifs (bottom) for small networks motifs ( $N = 2$ ) of Rössler systems coupled by their different variables. The root strongly connected components (rSCC) are shown in dashed lines.

When a single variable is measured ( $m = 1$ ), the pair  $[\mathcal{J}_N, \mathbf{X}]$  is always poorly observable, even when there is a single rSCC (via  $H_x$  or  $H_y$ ). The symbolic observability coefficients are very well confirmed by the determinants which are at least second-order polynomials (not shown).

When two variables are measured,  $m = 2$ , in just a single node,  $N_m = 1$ , full observability of the pair  $[\mathcal{J}_N, \mathbf{X}]$  is obtained only through  $H_y$ . We found three possibilities for the reconstructed state vector  $\mathbf{X}$  providing  $\eta_{\mathbf{X}} = 1$ . In these cases, the corresponding determinants depend on  $\rho_y^3$  (Table. 1). Such a strong dependency on the coupling strength could deteriorate the observability when  $\rho_y$  becomes small. On the other hand, when the two variables measured are coming from two different nodes, there is a wide variety of possibilities providing a fully observable pair  $[\mathcal{J}_N, \mathbf{X}]$ . There is a strong advantage of using variable  $y$  and its first two derivatives in each node since it provides a full observability and the determinant is not dependent on the coupling strength ( $\text{Det } \mathcal{O}_{\mathbf{X}} = 1$ ).

Among other possibilities offering full observability is that from the reconstructed vector  $\mathbf{X} = (x_1^2 y_2^4)$  (where the notation  $x_i^j$  designates the first  $j$  Lie derivatives of variable  $x_i$ , being the first one the variable itself), either using the coupling functions  $H_y$  or  $H_z$ . However, when looking at the corresponding determinants  $\Delta_{x_1^2 y_2^4} = \rho_y^3$  and  $\Delta_{x_1^2 y_2^4} = -\rho_z$  respectively, we unexpectedly notice that the observability depends on the coupling strength in a weaker way when nodes are coupled *via* variable  $z$  than *via* variable  $y$ . And even more surprising is the case when nodes are coupled *via* variable  $x$ , since the determinant (not shown in Table 1)  $\Delta_{x_1^2 y_2^4} = 0$ , indicating that the network is not observable at

**Table 1.** Symbolic observability coefficients  $\eta$  for the dyads shown in Fig. 2. The type of coupling function  $H$ , the number  $m$  of measured variables and the number of nodes  $N_m$  where they are measured are also reported. Analytical determinants are reported only in those cases when  $\eta = 1$ . To shorten the notation of the reconstructed vector, we used  $y^3$  instead of  $(y, \dot{y}, \ddot{y})$ , where the exponent refers to the number of derivatives (including the variable itself). The index is omitted when only the variable itself appears in the reconstruction vector.

$H$	$m = 1$	$m = 2, N_m = 1$	$m = 2, N_m = 2$
$H_x$	$\eta_{x^6} = 0.65$	$\eta_{y^5 z} = 0.91$	$\eta_{y_1^3 y_2^3} = 1$ (Det $\mathcal{O} = 1$ )
	$\eta_{y^6} = 0.41$		$\eta_{y_1^2 y_2^4} = 1$ (Det $\mathcal{O} = \rho_z$ )
	$\eta_{z^6} = 0.03$		$\eta_{x_1 y_2^5} = 0.91$ $\eta_{x_1^3 x_2^3} = 0.79$
$H_y$	$\eta_{x^6} = 0.66$	$\eta_{x^5 y} = 1$ (Det $\mathcal{O} = -\rho_y^3$ )	$\eta_{y_1^3 y_2^3} = 1$ (Det $\mathcal{O} = 1$ )
	$\eta_{y^6} = 0.56$	$\eta_{x^2 y^4} = 1$ (Det $\mathcal{O} = \rho_y^3$ )	$\eta_{y_1^2 y_2^4} = 1$ (Det $\mathcal{O} = -\rho_y$ )
	$\eta_{z^6} = 0.31$	$\eta_{x^5 z} = 1$ (Det $\mathcal{O} = \rho_y^3$ )	$\eta_{x_1^2 y_2^4} = 1$ (Det $\mathcal{O} = -\rho_y^3$ )
		$\eta_{y^4 z^2} = 0.86$	$\eta_{x_1^3 y_2^3} = 0.91$
		$\eta_{y^5 z} = 0.77$	$\eta_{x_1^3 x_2^3} = 0.91$
$H_z$	$\eta_{x^6} = 0.72$	$\eta_{x^5 y} = 0.72$	$\eta_{y_1^3 y_2^3} = 1$ (Det $\mathcal{O} = 1$ )
	$\eta_{y^6} = 0.37$	$\eta_{x^5 z} = 0.72$	$\eta_{y_1^2 y_2^4} = 1$ (Det $\mathcal{O} = -\rho_z$ )
	$\eta_{z^6} = 0.11$	$\eta_{x^2 z^4} = 0.72$	$\eta_{x_1^2 y_2^4} = 1$ (Det $\mathcal{O} = -\rho_z$ )
		$\eta_{y^2 z^4} = 0.72$	$\eta_{y_1 y_2^5} = 0.86$ $\eta_{x_1^3 x_2^3} = 0.79$

all. Consequently, the observability of our network with a given topology and reconstructed state vector  $\mathbf{X}$  strongly depends on the coupling variable.

Notice also that the graphical analysis of the pruned fluence graph of  $\mathcal{J}_N$  is providing a necessary condition about the variables to be measured for getting full observability but it may not be sufficient. For example, in Fig. 2b, it is recommending to measure either  $x$  or  $y$  from the single rSCC but to get full observability a second variable is needed. This leads to the following propositions.

**Proposition 1** *The minimal number  $m_{\min}$  of variables necessary to measure for getting full observability of a  $d \cdot N$ -dimensional network  $\mathcal{N}$  is equal to the number  $N_r$  of root strongly connected components. Each measured variable has to be chosen in a different root strongly connected component.*

**Corollary 1** *If additional variables are required to get a full observability of a  $d \cdot N$ -dimensional network, they will be selected in the  $N_r$  root strongly connected components and, preferably, in those whose cardinality is the largest.*

Thus, with these rules from the analysis of the pruned fluence graph, the number of vectors  $\mathbf{X}$  is sufficiently reduced to make exhaustive computations of the symbolic observability coefficients.

**Proposition 2** *When the node dynamics is fully observable from one of its variables, then the network  $\mathcal{N}$  is fully observable if that variable is measured at each node ( $m = N$ ), independently from the coupling function and topology, even when the network is not completely connected.*

**Corollary 2** *When the number  $N_m$  of measured nodes is such that  $N_m < N$ , by definition, the choice of the variables to measure is not only dependent on the adjacency matrix  $A$  and coupling function  $H$  but also on the node dynamics.*

**Proposition 3** *When a network  $\mathcal{N}$  of Rössler systems coupled by the variable  $z$ , then  $m = N$  nodes must be necessarily measured for getting full observability.*

#### 4.2 Triads ( $N = 3$ )

Let us now consider motifs of  $N = 3$  nodes. To limit the number of cases to discuss, we will analyze only triad networks coupled through variable  $y$  since this is the sole coupling configuration for which a dyad of Rösslers are fully observable from measurements in a single node (see Table 1). In order to refer to all the possible triad motifs shown in Fig. 3, we will distinguish them by the number  $l$  of directed edges,  $T_l$ , such that there are five classes of motifs:  $T_2$  (3),  $T_3$  (4),  $T_4$  (4),  $T_5$  (1), and  $T_6$  (1).

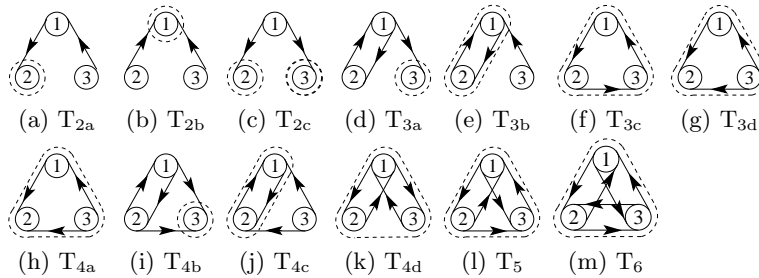


**Fig. 3.** Network connection motifs for triad networks ( $N = 3$ ) of Rössler systems coupled by variable  $x$  or  $y$ . Only the rSCCs are shown (dashed line).

Let us start with the triad  $T_{2a}$  shown in Fig. 3a. There is a single root strongly connected component comprised by the vertices  $x_2$  and  $y_2$ . According to this graph, measuring either  $x_2$  or  $y_2$  in node 2 should provide full observability of the triad  $T_{2a}$ . However, when two variables are measured in that node, the largest observability coefficient is  $\eta_{y_2^2 z_2} = 0.59$ . Measuring a third variable in node 2 does not improve the observability since the symbolic observability coefficient becomes null. The triad  $T_{2a}$  is therefore poorly observable when measurements are only performed in the rSCC. Therefore, a proposition is made as follows.

**Proposition 4** *In a network of  $N$  Rössler systems, it is not possible to reconstruct with full observability the space associated with three nodes from measurements in a single node.*



**Table 2.** Determinants of the observability matrix and symbolic observability coefficients for three of the triads shown in Fig. 3 and for different reconstructed vectors  $\mathbf{X}$ . Determinants with a polynomial of degree  $i$  dependence are indicated with  $P_i$ . The value of the observability coefficient with a \* is spurious due to symmetries in the observability matrix that cancel the determinant and that the symbolic formalism does not detect: it should be zero.

Triad	T <sub>2a</sub>	T <sub>4d</sub>	T <sub>6</sub>
$\mathbf{X} = (x_2^2, y_2^4, y_3^3)$	Det $\mathcal{O}_{\mathbf{X}} = -\rho_y^3$ $\eta_{\mathbf{X}} = 1$	Det $\mathcal{O}_{\mathbf{X}} = -\rho_y^3$ $\eta_{\mathbf{X}} = 1$	Det $\mathcal{O}_{\mathbf{X}} = -\rho_y^3$ $\eta_{\mathbf{X}} = 1$
$\mathbf{X} = (x_2^2, y_2^5, y_3^2)$	Det $\mathcal{O}_{\mathbf{X}} = -\rho_y^5$ $\eta_{\mathbf{X}} = 1$	Det $\mathcal{O}_{\mathbf{X}} = -\rho_y^5$ $\eta_{\mathbf{X}} = 1$	Det $\mathcal{O}_{\mathbf{X}} = \rho_y^4 P_1$ $\eta_{\mathbf{X}} = 0.88$
$\mathbf{X} = (x_2^2, y_2^6, y_3)$	Det $\mathcal{O}_{\mathbf{X}} = \rho_y^7 P_2$ $\eta_{\mathbf{X}} = 0.82$	Det $\mathcal{O}_{\mathbf{X}} = \rho_y^7 P_3$ $\eta_{\mathbf{X}} = 0.82$	Det $\mathcal{O}_{\mathbf{X}} = \rho_y^7 P_3$ $\eta_{\mathbf{X}} = 0.68$
$\mathbf{X} = (x_2^2, y_2^7)$	Det $\mathcal{O}_{\mathbf{X}} = 0$ $\eta_{\mathbf{X}} = 0.69^*$	Det $\mathcal{O}_{\mathbf{X}} = \rho_y^9 P_5$ $\eta_{\mathbf{X}} = 0.69$	Det $\mathcal{O}_{\mathbf{X}} = \rho_y^7 P_5$ $\eta_{\mathbf{X}} = 0.60$

Therefore, the nine dimensions of a Rössler triad can not be observed from just measuring in one node. However, from the dyad analysis, when the coupling function is via the  $y$  variable, it is possible to reconstruct the six associated dimensions from measurements ( $m = 2$ ) in a single node. In order to investigate what is the largest dimension that can be reconstructed, we consider the vector  $\mathbf{X} = (x_2^2, y_2^4, y_3^3)$  which provides full observability of the triad  $T_{2a}$  (Det  $\mathcal{O}_{\mathbf{X}} = -\rho_y^3$ ) by performing  $m = 3$  measurements, two in node 2 and one in node 3. Now, we proceed by progressively adding an extra Lie derivative of  $y_2$  and removing it from  $y_3$  until full observability is lost for  $\mathbf{X} = (x_2^2, y_2^7)$ . For the case  $\mathbf{X} = (x_2^2, y_2^5, y_3^2)$ , Det  $\mathcal{O}_{\mathbf{X}} = -\rho_y^5$  and therefore a full observable pair  $[\mathcal{J}_N, \mathbf{X}]$  is still obtained. However, one more Lie derivative of  $y_2$ ,  $\mathbf{X} = (x_2^2, y_2^6, y_3)$ , leads to Det  $\mathcal{O}_{\mathbf{X}} = -\rho_y^3 [(a + c - x_1)(x_1 - x_3) + y_1 + 2z_1 - z_3 - 1]$ , that is, observability is good since a singular observability manifold appears with this first-order determinant and  $\eta_{\mathbf{X}} = 0.82$ . Therefore, the largest dimension that can be reconstructed from measurements in a single Rössler node is six. The triads  $T_{4d}$  and  $T_6$  led to similar results (Table 2): full observability of a triad of Rösslers is only possible when no more than seven dimensions are reconstructed from measurements in a single node. As soon as eight dimensions are recovered from one node, the reconstructed vector provides poor observability of the whole system.

**Proposition 5** *In a network of Rössler systems, it is not possible to reconstruct with full observability more than two nodes from measurements in a single node.*

**Proposition 6** *When  $N > 2$  Rössler systems are coupled, full observability is only possible if at least  $N_m = \frac{N}{2} + (N \bmod 2)$  nodes are measured and  $m = N$  variables are measured.*

This proposition could be specific to the Rössler system or even be more generic. This will be further investigated elsewhere.

An additional question to address to complete the observability analysis of the triad is to check whether it is possible to reconstruct a node from another one not directly connected to it. Let us consider the triad  $T_{2a}$  and the reconstructed vector  $\mathbf{X} = (x_2^2, y_2^4, y_1^3)$  where  $m = 3$  measurements are performed in nodes 1 and 2. Note that in triad  $T_{2a}$  information is flowing from 3 to 2 through node 1 which is measured. The three extra dimensions reconstructed from node 2 cannot be used for node 3 (not directly connected) but only for node 1. Node 1 is thus observed twice, leading to  $\text{Det } \mathcal{O}_{\mathbf{X}} = 0$ : there is null observability of the triad  $T_{2a}$  from such a reconstructed vector  $\mathbf{X}$ . Contrary to this, the vector  $\mathbf{X} = (y_2^3, x_1^2, y_1^4)$  provides full observability of triad  $T_{2a}$ , node 3 being reconstructed from node 1. Then, we state the following proposition.

**Proposition 7** *A necessary condition for having full observability of a non measured node  $n_i$  from a measured one  $n_j$  is that there is an edge from  $n_i$  to  $n_j$ .*

**Corollary 3** *If the node dynamics is a Rössler system, a non measured node can be fully observable if it is directly coupled via variable  $y$  to a measured one.*

## 5 Larger networks

### 5.1 Star network

Let us consider a star network of  $N$  nodes, being  $N - 1$  of them leaves and one acting as the hub. The number  $N_r$  of rSCCs depends on the number  $l$  of edges and how these edges are directed. When couplings are bidirectional, there is a single rSCC that contains all the nodes. When unidirectional couplings are all directed to the hub, the hub is the rSCC. When all the edges are out-going from the hub, there are  $N_r = N - 1$  rSCC, each one made of one leaf. In a random star network with  $N_{\text{out}}$  edges out-going from the hub, there are  $N_{\text{out}}$  rSCCs, each one made of one of the leaves receiving one of these out-going edges. In all cases, according to propositions 1 and 5,  $m = N$  variables must be measured in  $N_m = N_r$  nodes.

### 5.2 Ring network

In a ring network of Rössler systems coupled *via* variable  $y$ , according to propositions 1 and 5,  $m = N$  variables must be measured in  $N_m = \frac{N}{2} + (N \bmod 2)$  nodes for full observability of the pair  $[\mathcal{J}_N, \mathbf{X}]$ . This result does not depend on the directionality of the edges (they can be either bidirectional or unidirectional). Along the ring, one in two nodes are measured.

### 5.3 Random network ( $N = 28$ )

We here investigate a random network made of 28 Rössler systems bidirectionally coupled *via* variable  $y$  according to the topology (Fig. 4) of an electronic network [14]. Applying propositions 1 and 5, nodes are grouped by pairs depending on

their edges. One possibility is to measure  $m = N + 1$  variables in 15 nodes, namely in nodes 1, 2, 3, 4, 5, 6, 7, 8, 9, 10, 13, 14, 15, 19, and 23. Measurements are needed in  $N_m = \frac{N}{2} + 1$  since two nodes, 22 and 23, are only connected to node 1, from which it is not possible to reconstruct three nodes according to proposition 4. One of these two nodes must also be measured. In all nodes but nodes 19 and 23, the reconstructed vector is  $\mathbf{X}_i = (x_i^2, y_i^4)$  while in nodes 19 and 23  $\mathbf{X}_j = y_j^3$ . The symbolic coefficient was equal to one and the analytical determinant of the observability matrix is  $\text{Det } \mathcal{O}_{\mathbf{X}} = \rho_y^{39}$ , therefore validating all our results. The expression of this determinant could mean that the observability is strongly sensitive to the coupling value. Nevertheless, since nodes are grouped by pair, the dependency on the coupling value should not be practically worse than the one observed for a pair of nodes, that is, depending on  $\rho_y^3$ .

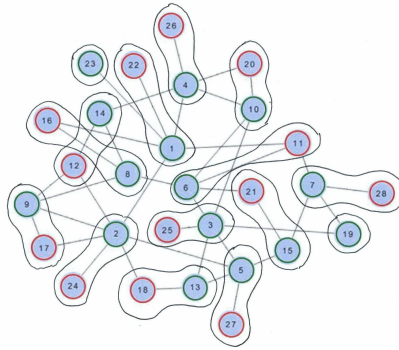


**Fig. 4.** Topology of the random network ( $N = 28$ ) used in Ref. [14] to implement a network of electronic Rössler-like circuits. Nodes are grouped by pairs to get full observability of this network from measurements in  $N_m = 15$  nodes.

## 6 Conclusion

We showed that it is possible to construct a procedure to reliably determine the observability of networks whose node dynamics are structurally identical (the governing equations have the same functional form but parameter values can differ). A reduced set of variables to measure in a network of  $N$  nodes and providing a full observability of it can be selected using a graphical approach [7]. Then symbolic coefficients are computed to quantify the observability of the network dynamics provided by the measurements [8]. To be fully reliable, network observability must be investigated from the complete Jacobian matrix  $\mathcal{J}_N$  of the network which encodes the topology, the coupling function and the node dynamics. Nevertheless, some systematic rules for assessing the observability of the network can be derived from the node Jacobian matrix  $\mathcal{J}_n$  and the coupling function of dyads and triads. First we determine the observability of the node dynamics. Then, using the results obtained from the analysis of a dyad, general

rules can be established to be applied to larger networks. In the case of Rössler systems, it is not possible to reconstruct more than two nodes from measurements in one node. It is necessary to measure at least in  $\frac{N}{2} + (N \bmod 2)$  nodes for getting full observability of a network made of  $N$ -Rössler systems coupled *via* variable  $y$ . For any other coupling,  $N$  nodes have to be measured. Therefore, the coupling function may critically affect the network observability.

## Acknowledgments

ISN acknowledges partial support from the Ministerio de Economía y Competitividad of Spain under project FIS2017-84151-P and from the Group of Research Excellence URJC-Banco de Santander.

## References

1. Bianchin, G., Frasca, P., Gasparri, A., Pasqualetti, F.: The observability radius of networks. *IEEE Transactions on Automatic Control* **62**(6), 3006–3013 (2017).
2. Chan, B.Y., Shachter, R.D.: Structural controllability and observability in influence diagrams. In: *Proceedings of the Eighth International Conference on Uncertainty in Artificial Intelligence*. pp. 25–32. UAI’92, Morgan Kaufmann Publishers Inc., San Francisco, CA, USA (1992)
3. Hasegawa, T., Takaguchi, T., Masuda, N.: Observability transitions in correlated networks. *Physical Review E* **88**, 042809 (2013).
4. Hermann, R., Krener, A.: Nonlinear controllability and observability. *IEEE Transactions on Automatic Control* **22**(5), 728–740 (1977).
5. Letellier, C., Aguirre, L.A.: Investigating nonlinear dynamics from time series: The influence of symmetries and the choice of observables. *Chaos* **12**(3), 549–558 (2002).
6. Letellier, C., Aguirre, L.A., Maquet, J.: Relation between observability and differential embeddings for nonlinear dynamics. *Physical Review E* **71**(6), 066213 (2005).
7. Letellier, C., Sendiña-Nadal, I., Aguirre, L.A.: A nonlinear graph-based theory for dynamical network observability. *Physical Review E* **98**, 020303(R) (2018).
8. Letellier, C., Sendiña-Nadal, I., Bianco-Martinez, E., Baptista, M.S.: A symbolic network-based nonlinear theory for dynamical systems observability. *Scientific Reports* **8**, 3785 (2018).
9. Lin, C.T.: Structural controllability. *IEEE Transactions on Automatic Control* **19**(3), 201–208 (1974).
10. Liu, Y.Y., Slotine, J.J., Barabási, A.L.: Observability of complex systems. *Proceedings of the National Academy of Sciences* **110**(7), 2460–2465 (2013).
11. Sendiña Nadal, I., Boccaletti, S., Letellier, C.: Observability coefficients for predicting the class of synchronizability from the algebraic structure of the local oscillators. *Physical Review E* **94**(4), 042205 (2016).
12. Newman, M.E.: *Networks: an introduction*. Oxford University Press, Oxford (2010)
13. Rössler, O.E.: An equation for continuous chaos. *Physics Letters A* **57**(5), 397–398 (1976).
14. Sevilla-Escoboza, R., Buldú, J.M.: Synchronization of networks of chaotic oscillators: Structural and dynamical datasets. *Data in Brief* **7**, 1185–1189 (2016).
15. Van Mieghem, P., Wang, H.: The observable part of a network. *IEEE/ACM Transactions in Networks* **17**(1), 93–105 (2009).